

# Hydrogen Bond Lifetimes and Energetics for Solute/Solvent Complexes Studied with 2D-IR Vibrational Echo Spectroscopy

Junrong Zheng and Michael D. Fayer\*

Contribution from the Department of Chemistry, Stanford University, Stanford, California 94305

Received November 3, 2006; E-mail: fayer@stanford.edu

**Abstract:** Weak  $\pi$  hydrogen-bonded solute/solvent complexes are studied with ultrafast two-dimensional infrared (2D-IR) vibrational echo chemical exchange spectroscopy, temperature-dependent IR absorption spectroscopy, and density functional theory calculations. Eight solute/solvent complexes composed of a number of phenol derivatives and various benzene derivatives are investigated. The complexes are formed between the phenol derivative (solute) in a mixed solvent of the benzene derivative and  $\text{CCl}_4$ . The time dependence of the 2D-IR vibrational echo spectra of the phenol hydroxyl stretch is used to directly determine the dissociation and formation rates of the hydrogen-bonded complexes. The dissociation rates of the weak hydrogen bonds are found to be strongly correlated with their formation enthalpies. The correlation can be described with an equation similar to the Arrhenius equation. The results are discussed in terms of transition state theory.

## I. Introduction

Hydrogen bonds play important roles in chemistry and biology.<sup>1–5</sup> Most hydrogen bonds have dissociation enthalpies in the range of 1–10 kcal/mol. This range is much smaller than a typical covalent bond enthalpy. For instance, a carbon–carbon single bond has a dissociation enthalpy of  $\sim 80$  kcal/mol.<sup>1</sup> In spite of being relatively weak, hydrogen bonds are strong enough to have a profound influence on the nature of liquids and material, and on the reactivity of hydrogen-bonded molecules. An important example is water, which is a liquid at room temperature rather than a gas because of its hydrogen-bond network. Another important aspect of hydrogen bonds is that they are weak enough that they can continually dissociate and reform at room temperature. Some of the most significant biological processes, such as DNA replication and protein folding, are made possible because of the reversible nature of hydrogen-bond formation.<sup>4</sup>

The reversibility of hydrogen bonding brings up two interesting and fundamental questions. (1) How long does a hydrogen bond stay “bonded” at room temperature? (2) Is there any correlation between the hydrogen bond lifetime and its strength? In general, it might be expected that stronger hydrogen bonds would dissociate more slowly. However, direct experimental data addressing these issues for relatively weak hydrogen bonds that can readily dissociate at room temperature are rare because there has been a lack of appropriate measurement techniques.

For some strong hydrogen bonds that have dissociation enthalpies greater than 5 kcal/mol, the hydrogen bond lifetimes are sufficiently long that they can be measured with temperature-jump or ultrasonic methods.<sup>2</sup> Measurements of the lifetimes of relatively weak hydrogen bonds ( $< 5$  kcal/mol) at room temperature under thermal equilibrium conditions have recently become possible because of the advent of ultrafast IR techniques.<sup>6–11</sup> To the best of our knowledge, no systematic study on the relationship between the lifetimes and strength of hydrogen bonds has been reported.

In this paper, we present a study of the lifetimes of hydrogen bonds between a series of phenol derivatives and benzene derivatives using the recently developed method of ultrafast 2D-IR vibrational echo chemical exchange spectroscopy.<sup>9–15</sup> The experiments described here follow previous work that examined the hydrogen-bond formation and dissociation rates of the phenol/benzene complex in liquid solution of low concentration phenol in the mixed benzene/ $\text{CCl}_4$  solvent.<sup>9,10</sup> A phenol molecule forms a weak hydrogen bond, sometimes called “ $\pi$  hydrogen bond,” with a benzene molecule. By adding different substituents to either phenol or benzene, the strength of the hydrogen bond can be modified. Using the 2D vibrational echo chemical exchange technique, the dissociation times of a series

- (1) Vinogradov, S. N.; Linnell, R. H. *Hydrogen Bonding*; Van Nostrand Reinhold Company: New York, 1971.
- (2) Joesten, M. D.; Schaad, L. J. *Hydrogen Bonding*; Marcel Dekker, Inc.: New York, 1974.
- (3) Jeffrey, G. A. *An Introduction to Hydrogen Bonding*; Oxford University Press, Inc.: New York, 1997.
- (4) Desiraju, G. R.; Steiner, T. *The Weak Hydrogen Bond*; Oxford: New York, 1999.
- (5) Pimentel, G. C.; McClellan, A. L. *Annu. Rev. Phys. Chem.* **1971**, *22*, 347–385.

- (6) Arrivo, S. M.; Heilweil, E. J. *J. Phys. Chem.* **1996**, *100*, 11975.
- (7) Arrivo, S. M.; Kleiman, V. D.; Dougherty, T. P.; Heilweil, E. J. *Opt. Lett.* **1997**, *22*, 1488–1490.
- (8) Woutersen, S.; Mu, Y.; Stock, G.; Hamm, P. *Chem. Phys.* **2001**, *266*, 137–147.
- (9) Zheng, J.; Kwak, K.; Asbury, J. B.; Chen, X.; Piletic, I.; Fayer, M. D. *Science* **2005**, *309*, 1338–1343.
- (10) Zheng, J.; Kwak, K.; Chen, X.; Asbury, J. B.; Fayer, M. D. *J. Am. Chem. Soc.* **2006**, *128*, 2977–2987.
- (11) Kim, Y. S.; Hochstrasser, R. M. *Proc. Natl. Acad. Sci. U.S.A.* **2005**, *102*, 11185–11190.
- (12) Zheng, J.; Kwak, K.; Xie, J.; Fayer, M. D. *Science* **2006**, *313*, 1951–1955.
- (13) Zheng, J.; Kwak, K.; Fayer, M. D. *Acc. Chem. Res.* **2006**, *40*, 75–83.
- (14) Kwak, K.; Zheng, J.; Cang, H.; Fayer, M. D. *J. Phys. Chem. B* **2006**, *110*, 19998–20013.
- (15) Sanda, F.; Mukamel, S. *J. Chem. Phys.* **2006**, *125*, 014507.

of hydrogen-bonded complexes are measured. In addition, temperature-dependent FT-IR absorption experiments are used to determine the formation enthalpies of the hydrogen bonds, and DFT calculations provide reasonable estimates of their structures. The results show a systematic correlation between the hydrogen-bond strengths (formation enthalpy) and the hydrogen-bond dissociation times.

## II. Experimental Procedures

Details of the experimental method used for these 2D-IR vibrational echo spectroscopy experiments have been described previously<sup>10,16</sup> and are also included in the Supporting Information for the convenience of the readers. In addition, a diagram of the experimental setup and a schematic representation of how the 2D vibrational echo method is used to measure chemical exchange are provided in the Supporting Information. Very briefly, in a 2D-IR vibrational echo chemical exchange experiment, three ultrashort IR pulses tuned to the frequency range of the vibrational modes of interest are crossed in the sample. Because the pulses are very short, they have broad bandwidths (determined by the uncertainty principle) making it possible to simultaneously excite a number of vibrational bands. The first laser pulse places the vibrational oscillators in coherent superposition states of the ground state (0) and the first excited state (1) and “labels” the initial structures of the species in the sample by setting their initial frequencies along the  $\omega_\tau$  axis. The second pulse ends the first time period  $\tau$  by transforming the coherences into populations (either in the 0 or 1 states) and starts clocking the reaction time period  $T_w$  during which the labeled species undergo chemical exchange, that is hydrogen-bond formation and dissociation. The chemical exchange will be manifested in the 2D spectrum if it changes the vibrational frequencies of the vibrational modes under study. The third pulse ends the population period of length  $T_w$  and begins a third period of length  $\leq \tau$ , which ends with the emission of the vibrational echo pulse with frequencies along the  $\omega_m$  axis. The vibrational echo pulse is the signal in the experiment. The vibrational echo signal reads out information about the final structures of all labeled species by their  $\omega_m$  frequencies. During the period  $T_w$  between pulses 2 and 3, chemical exchange occurs. The exchange causes new off-diagonal peaks to grow in as  $T_w$  is increased.<sup>9–12</sup> The growth of off-diagonal peaks in the 2D spectra with increasing  $T_w$  is used to extract the dissociation times (lifetimes) of the hydrogen bonds. (Chemical exchange can also occur during the  $\tau$  periods, but it does not contribute to the growth of the off-diagonal peaks.) In addition to chemical exchange, other population dynamics such as vibrational relaxation to the ground state and orientational relaxation of the entire molecule will influence the 2D spectrum. These processes are included in the data analysis.

The vibrational population relaxation time constants and rotational relaxation time constants for the samples were measured with the polarization selective IR pump–probe experiments.<sup>10,17</sup> The rotational relaxation time constants were measured in the pure solvents. The value measured in  $\text{CCl}_4$  was used to determine the rotational time of the free (uncomplexed) species, and the value measured in the pure aromatic solvent was used to determine the rotational time of the complex. These values were corrected with the Stokes–Einstein–Debye (SED) equation for the solvent viscosity differences between the pure aromatic solvent or  $\text{CCl}_4$  and the mixed solvents used in the chemical exchange experiments. Viscosity measurements were made with Cannon Ubbelohde viscometers at 24 °C, the same temperature used for the vibrational echo and pump–probe measurements.

The hydrogen-bond formation enthalpies of the complexes were determined by measuring the temperature dependence of the equilibrium constant by observing the change in the absorption spectrum of the hydroxyl stretching mode. The ratio of the areas of the peaks for the

complex species and the free species, corrected for the differences in extinction coefficients, was used to determine the equilibrium constant at each temperature. The temperature range was 25 to 65 °C. A more detailed description of the measurements and experimental data are given in the Supporting Information.

The hydroxyl groups of all phenol derivatives were deuterated to move the hydroxyl stretching mode frequency to  $\sim 2600 \text{ cm}^{-1}$ . The chemicals used to form the hydrogen-bonded complexes are phenol-OD (PH), *p*-methoxyphenol-OD (pMPH), *p*-bromophenol-OD (pBrPH), *o*-methoxyphenol-OD (oMPH), benzene (BZ), toluene (TL), bromobenzene (BrBZ), *p*-xylene (pX), and mesitylene (MS). The solutions used in the vibrational echo measurements are 0.6 wt % PH in the BZ/ $\text{CCl}_4$  mix solvent (1:5 wt), 0.6 wt % PH in TL/ $\text{CCl}_4$  (1:6 wt), 0.6 wt % PH in pX/ $\text{CCl}_4$  (1:7 wt), 0.6 wt % PH in MS/ $\text{CCl}_4$  (1:7 wt), 0.6 wt % pBrPH in BZ/ $\text{CCl}_4$  (1:5 wt), 0.5 wt % pMPH in BZ/ $\text{CCl}_4$  (1:5 wt), and 3 wt % oMPH in TL. The ratio of the aromatic component of the solvent to the  $\text{CCl}_4$  component was chosen to make free and complexed species approximately equal in amplitude in the FTIR spectrum of each mixture.

The function of the substituents on the phenol and benzene rings is to adjust the hydrogen-bond strength (enthalpy of formation). Benzene and its derivatives are the hydrogen-bond acceptors. In general, adding an electron-withdrawing group such as bromine to benzene weakens the hydrogen bond by reducing the electron density of the benzene ring. Adding electron-donating groups such as methyl groups to benzene makes the hydrogen bond stronger. Adding an electron-withdrawing group to phenol also makes the hydrogen bond stronger because the hydroxyl, which is the hydrogen bond donor, becomes more positive. The effect of a methoxy group on the phenol ring is position dependent. When it is ortho to the hydroxyl, the hydroxyl group forms an intramolecular hydrogen bond with the methoxy group. The intramolecular hydrogen bond results in an intermolecular  $\pi$  hydrogen bond between the hydroxyl group and aromatic solvent molecule that is very weak.<sup>10</sup> When the methoxy group is in the para position, it has very little effect on the strength of the intermolecular hydrogen bond.

The structures of the hydrogen-bonded complexes were determined with density functional theory (DFT) calculations.<sup>18</sup> The DFT calculations were carried out as implemented in the Gaussian 98 program suite. The level and basis set used were Becke’s three-parameter hybrid functional combined with the Lee–Yang–Parr correction functional, abbreviated as B3LYP, and 6-31+G(d,p). All results reported here do not include the surrounding solvent and therefore are for the isolated molecular complexes.

## III. Results and Discussions

The DFT calculations show that all of the phenol derivatives form  $\pi$  hydrogen bonds with the aromatic molecules in the mixed solvents and that all of the complexes have a similar T-shaped structure. The structure is shown in Figure 1 for the phenol/toluene complex. Structures for other complexes are provided in the Supporting Information. For the phenol/benzene complex, recent high-level electronic structure calculations on the isolated complex and full molecular dynamic simulations of PH in the BZ/ $\text{CCl}_4$  solvent confirm the T-shape structure.<sup>19</sup> In addition, the simulations show that the complexes are formed one to one between PH and BZ. The hydroxyl group does not point at the center of the benzene ring but rather at a ring edge for all the systems studied. The structures of the complexes in solution can be different from those predicted by the electronic structure calculations for isolated molecules. However, the consistency between the electronic structure calculations and

(16) Asbury, J. B.; Steinel, T.; Fayer, M. D. *J. Lumin.* **2004**, *107*, 271–286.  
(17) Tan, H. S.; Piletic, I. R.; Fayer, M. D. *J. Chem. Phys.* **2005**, *122*, 174501.

(18) Parr, R. G.; Yang, W. *Density Functional Theory of Atoms and Molecules*; Oxford University Press: New York, 1989.  
(19) Kwac, K.; Lee, C.; Jung, Y.; Han, J.; Kwak, K.; Zheng, J.; Fayer, M. D.; Cho, M. *J. Chem. Phys.* **2006**, *125*, 244508.

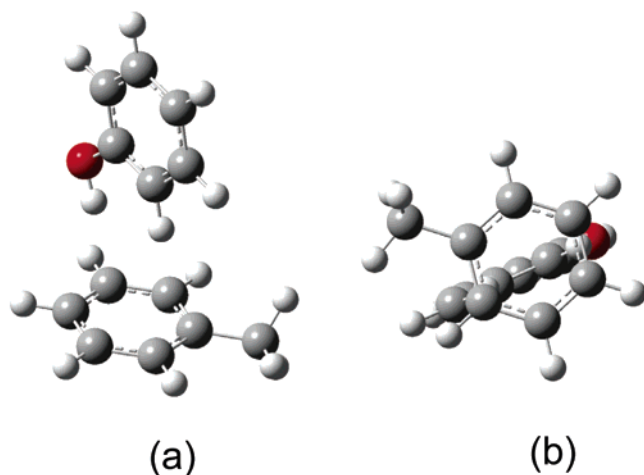


**Figure 1.** Two views of the hydrogen-bonded structure of the phenol/toluene complex calculated with DFT at the B3LYP/6-31+G(d,p) level for the isolated molecules. The complex's binding energy is found to be  $-2.3$  kcal/mol (with zero-point energy correction) without solvent interactions.

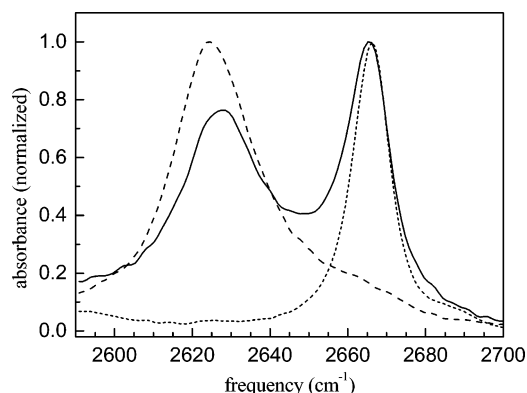


**Figure 2.** FT-IR absorption spectra of the OD stretch of phenol-OD (hydroxyl H replaced with D) in  $\text{CCl}_4$  (free phenol, dotted curve), phenol in toluene (hydrogen-bonded phenol/toluene complex, dashed curve), and phenol in the mixed toluene/ $\text{CCl}_4$  solvent, which displays absorptions for both free and complexed phenol (solid curve).

the simulations for the PH/BZ system suggests that the electronic structure calculations for the other complexes provide a reasonable description of their structures.

Experimental evidence for the formation of  $\pi$  hydrogen bonds is the shift of the OD stretch frequency of the phenol derivatives to lower frequencies in aromatic solvents compared to the corresponding frequencies of the phenols in  $\text{CCl}_4$ . Figure 2 displays FT-IR spectra for PH dissolved in pure  $\text{CCl}_4$  (short dash), pure TL (long dash), and the mixed TL/ $\text{CCl}_4$  solvent (solid curve).

When phenol is dissolved in  $\text{CCl}_4$ , there is no hydrogen bond formed. The OD stretch frequency is at  $2666\text{ cm}^{-1}$ . When it is dissolved in toluene, a hydrogen-bonded complex is formed between a solute and a solvent molecule. The OD stretch frequency red-shifts to  $2625.6\text{ cm}^{-1}$ . When phenol is dissolved in the TL/ $\text{CCl}_4$  mixture, some of the phenol molecules form complexes with toluene and some of them are free. The free and complexed phenol molecules are in dynamic equilibrium. As we can see from the spectrum, in the mixed solvent both free phenol and the phenol/toluene complex are present.

It is well-known that hydrogen bonding shifts the hydroxyl stretch frequency to a lower frequency and that stronger

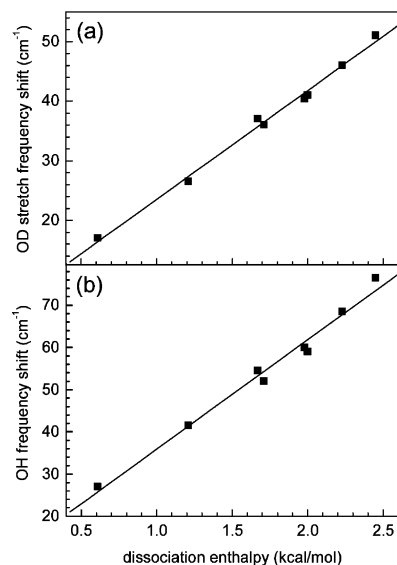


**Figure 3.** Correlation between the frequency shift (relative to the free species) of (a) OD stretch and (b) OH stretch of complexes of phenol and its derivatives to benzene derivatives and the complex (hydrogen bond) dissociation enthalpies (negative values of formation enthalpies). The two plots show a linear relationship between the parameters.

hydrogen bonds produce greater shifts.<sup>5,20–22</sup> For the complexes studied here, the hydroxyl stretch frequency shifts (relative to each corresponding free species) are also strongly correlated to the strength of the hydrogen bonds. Figure 3 shows that the frequency shift is linearly proportional to the hydrogen-bond dissociation enthalpy (negative of the formation enthalpy) for both the OD stretch with

$$\Delta\nu\text{ (cm}^{-1}\text{)} = 18.2 \times \Delta H\text{ (kcal/mol)} + 5.2 \quad (1)$$

and the OH stretch with

$$\Delta\nu\text{ (cm}^{-1}\text{)} = 25.9 \times \Delta H\text{ (kcal/mol)} + 10.0 \quad (2)$$

These results are similar to some other hydrogen-bonded systems.<sup>2,21,22</sup> The frequency shifts and enthalpy values are listed in Table 1.

The linear IR absorption measurements provide equilibrium thermodynamic data for the  $\pi$  hydrogen-bonded complexes. However, such measurements do not provide information regarding the complex dynamics, that is the dissociation and formation rates. Nonlinear 2D-IR experiments on the hydroxyl stretch permit direct determinations of these rates. The phenol in toluene/ $\text{CCl}_4$  system will be used to demonstrate the manner in which the hydrogen bond lifetimes (complex dissociation rates) can be extracted from the vibrational echo 2D-IR chemical exchange measurements. The hydrogen bond lifetimes for all of the other systems are obtained in the same manner.

Figure 4 displays 2D-IR spectra for a very short reaction period,  $T_w = 200$  fs (left panel) and a longer period,  $T_w = 12$  ps (right panel). The data have been normalized to the largest peak for each  $T_w$ . Each contour represents a 10% change in amplitude. (The data has 2% amplitude resolution. The 10% contours are shown here for clarity.) In Figure 4, only the 0–1

(20) Pimentel, G. C.; McClellan, A. L. *The Hydrogen Bond*; W. H. Freeman and Co.: San Francisco, 1960.

(21) Murphy, A. S. N.; Rao, C. N. R. *Appl. Spectrosc. Rev.* **1968**, *2*, 69–191.

(22) Lopes, M. C. S.; Thompson, H. W. *Spectrochim. Acta, Part A* **1968**, *24*, 1367–1383.

**Table 1.** Hydrogen Bond Lifetimes,  $\tau_d = 1/k_d$ , Bond Formation Enthalpies<sup>a</sup> ( $\Delta H^0$ ), Bond Formation Entropies ( $\Delta S^0$ ),<sup>b</sup> OH and OD Stretch Frequency Shifts of the Hydrogen-Bonded Phenol Derivatives (Relative to the Free Species)

	oMPH/TL	PH/BrBZ	PH/BZ	pMPH/BZ	PH/TL	BrPH/BZ	PH/pX	PH/MS
$\tau_d$ (ps)	3 ± 1	6 ± 3	10 ± 3	10 ± 3	15 ± 3	17 ± 2	24 ± 3	31 ± 4
$\Delta H^0$ (kcal/mol)	-0.6	-1.2	-1.7	-1.7	-2.0	-2.0	-2.2	-2.45
$\Delta S^0$ (J/mol K)	-30	-36	-34	-38	-8	-38	-34	-41
OH $\Delta\nu$ (cm <sup>-1</sup> )	27	41.5	54.5	52	60	59	68.5	76.5
OD $\Delta\nu$ (cm <sup>-1</sup> )	17	26.5	37	36	40.4	41	46	51

<sup>a</sup> The  $\Delta H^0$  values are relative to phenol in CCl<sub>4</sub>. The hydrogen-bond formation enthalpy between phenol and CCl<sub>4</sub> was determined to be  $\sim 0$  kcal/mol using anisole as the solvation model compound.<sup>35</sup> <sup>b</sup> The enthalpy error bars are  $\pm 0.2$  kcal/mol. The frequency error bars are  $\pm 0.5$  cm<sup>-1</sup>.

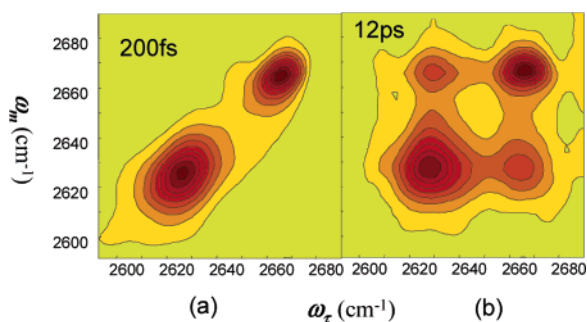


**Figure 4.** 2D-IR vibrational echo spectra of the OD stretch of phenol in the mixed toluene/CCl<sub>4</sub> solvent (only 0–1 transition data are shown). The data have been normalized to the largest peak for each  $T_w$ . Each contour represents 10% change in amplitude. (a) Data for  $T_w = 200$  fs. (b) Data for  $T_w = 12$  ps. At the longer time, additional peaks have grown in because of chemical exchange, that is, the formation and dissociation of the hydrogen-bonded complex of phenol and toluene.

(OD stretch vibrational ground state to the first excited state) transition portions of the spectra are shown. Spectra including both 0–1 and 1–2 transitions for all samples are provided in the Supporting Information. For  $T_w = 200$  fs, a short time compared to the exchange time (inverse of the hydrogen-bond dissociation and formation rates), the 2D-IR spectrum consists of two peaks on the upper-right to lower-left diagonal. These peaks arise from the 0–1 transitions of the free and hydrogen-bonded OD stretch (see Figure 2 solid curve). The two peaks are generated in the following manner. As described in the Experimental Procedures section, the first laser pulse simultaneously labels the initial structures of both free and hydrogen-bonded phenol molecules with the initial frequencies  $\omega_\tau$  (the OD stretch frequencies of both species). No exchange has occurred during the 200 fs  $T_w$  period. None of the “labeled” species has changed its structure, so the final frequency,  $\omega_m$ , detected by the vibrational echo is the same as the initial excitation frequency,  $\omega_\tau$ . If the initial frequency ( $\omega_\tau$ ) is the same as the final frequency ( $\omega_m$ ), the peak is on the diagonal. Therefore, for very short  $T_w$ , there are two diagonal peaks in the 2D-IR spectrum, one peak for the complex and one peak for the free phenol. The complex gives rise to the lower-frequency peak along the  $\omega_m$  axis because it is the lower-frequency peak in the linear IR spectrum (Figure 2). Within experimental error, both peaks in the 2D spectrum have the same frequencies as those in the FT-IR spectrum in Figure 2.

For  $T_w = 12$  ps (Figure 4, right panel), which is long compared to the exchange time for this system, two off-diagonal peaks have grown in. The growth of the additional peaks is caused by the exchange during  $T_w$  period. Consider phenols that are complexed with toluenes at the time of the second pulse. During the  $T_w$  period, some of these complexed phenols ( $\omega_\tau = 2625.6$  cm<sup>-1</sup>) dissociate, while some remain complexed. The third laser pulse ends the  $T_w$  period. The initially complexed

phenols have two possible final structures: free phenol molecules that produce the off-diagonal peak ( $\omega_\tau = 2625.6$  cm<sup>-1</sup>,  $\omega_m = 2666$  cm<sup>-1</sup>) and complexed phenols that still produce the diagonal peak (2625.6 cm<sup>-1</sup>, 2625.6 cm<sup>-1</sup>, respectively). Note that the peaks are determined only by the initial and final structures. Any odd number of exchanges, 1, 3, ..., etc., will produce an off-diagonal peak, and any even number of exchanges, 0, 2, ..., etc., will give rise to a diagonal peak. The same reasoning applies to initially free phenols which give rise to the free phenol diagonal peak and the other off-diagonal peak. The discussion here is for the slow exchange limit. For fast exchange, a single peak would be observed in the FT-IR spectrum.<sup>23</sup> In the slow exchange limit, the small amount of exchange that occurs during the  $\tau$  periods causes a reduction in the signal but does not give rise to off-diagonal peaks.<sup>14</sup> All the systems studied here are in the slow exchange limit.

Figure 5 displays  $T_w$ -dependent 2D-IR vibrational echo spectra for the hydroxyl stretch 0–1 transition region of the phenol/toluene/CCl<sub>4</sub> system. Each contour represents a 10% change in amplitude of the peaks. The growth of the off-diagonal peaks is evident as  $T_w$  increases from 200 fs (a short time compared to time for exchange) to 12 ps, at which time extensive exchange has occurred. Without any analysis, it is clear that the exchange time is slower than  $\sim 1$  ps and faster than  $\sim 100$  ps. However, to obtain quantitative rates requires a full analysis of the dynamical processes in the system.

During the  $T_w$  period, in addition to chemical exchange other dynamic processes influence the 2D spectrum. These are spectral diffusion, orientational relaxation, and vibrational relaxation.<sup>9,14</sup> None of these produce off-diagonal peaks. Spectral diffusion<sup>24,25</sup> is the result of time-dependent interactions of the vibrational transition with the solvent.<sup>14,26,27</sup> These interactions cause the transition frequency to fluctuate. At short time, the diagonal peaks' line shapes measured in the 2D vibrational echo spectrum are elongated along the diagonal because molecules are in different solvent environments (inhomogeneous broadening). As  $T_w$  increases, the solvent configurations around each molecule evolve so that the frequency of each molecule samples an increasingly large fraction of the entire absorption spectrum (spectral diffusion). At sufficiently long  $T_w$ , all possible solvent configurations are sampled, and the dynamic line width is equal to the absorption line width. In a 2D spectrum complete spectral diffusion is manifested by a change in the 2D line shape from elongated along the diagonal to symmetrical about the diagonal.

(23) Levinger, N. E.; Davis, P. H.; Behera, P.; Myers, D. J.; Stromberg, C.; Fayer, M. D. *J. Chem. Phys.* **2003**, *118*, 1312–11326.

(24) Walsh, C. A.; Berg, M.; Narasimhan, L. R.; Fayer, M. D. *Chem. Phys. Lett.* **1986**, *130*, 6–11.

(25) Bai, Y. S.; Fayer, M. D. *Phys. Rev. B* **1989**, *39*, 11066.

(26) Asbury, J. B.; Steinel, T.; Stromberg, C.; Corcelli, S. A.; Lawrence, C. P.; Skinner, J. L.; Fayer, M. D. *J. Phys. Chem. A* **2004**, *108*, 1107–1119.

(27) Asbury, J. B.; Steinel, T.; Kwak, K.; Corcelli, S.; Lawrence, C. P.; Skinner, J. L.; Fayer, M. D. *J. Chem. Phys.* **2004**, *121*, 12431–12446.

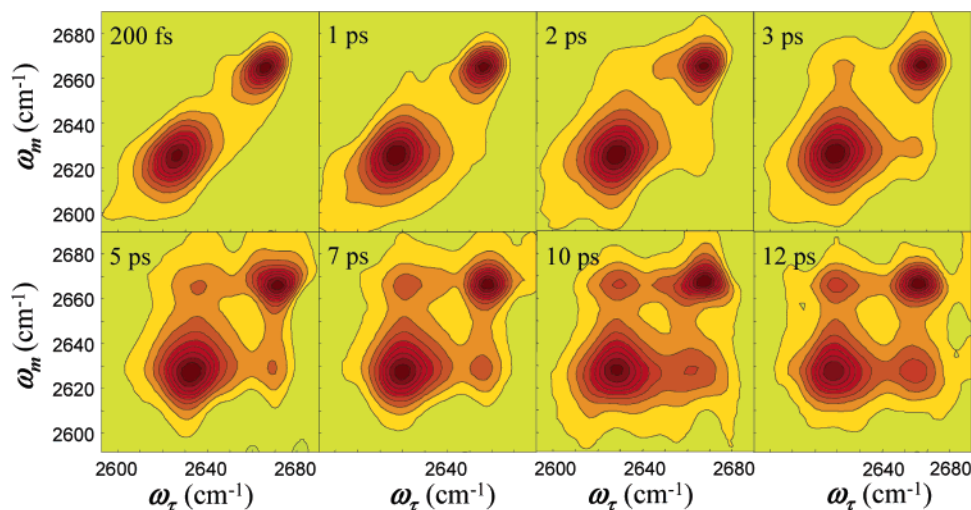
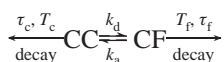


**Figure 5.** Time dependence of the 2D-IR vibrational echo spectrum in the 0–1 transition region. The data have been normalized to the largest peak for each  $T_w$ . Each contour represents 10% change in amplitude. As  $T_w$  increases, the off-diagonal peaks grow in because of chemical exchange (formation and dissociation of the toluene/phenol complex). Inspection of the data shows that the time scale for the chemical exchange (growth of the off-diagonal peaks) is a few picoseconds.

This change can be seen most clearly by comparing the central contours of the free peaks at 200 fs and 2 ps in Figure 5. Spectral diffusion changes the shapes of the peaks but preserves their volumes.<sup>9,14</sup> From the data, we can see that spectral diffusion is complete by  $\sim 2$  ps. Orientational relaxation and vibrational relaxation causes all peaks to decay in volume in contrast to chemical exchange, which causes the off-diagonal peaks to grow and the diagonal peaks to shrink. Orientational relaxation during the  $T_w$  period reduces the peak volumes but does not cause them to decay to zero. Vibrational relaxation does cause the peaks to eventually decay to zero.

To extract the exchange kinetics from the 2D-IR spectra, a kinetic model including all dynamic processes was used.<sup>9,10,14</sup> The method is illustrated schematically for the complex (CC) dissociating to become (CF) free phenol (or a phenol derivative).



CC represents the complexes (hydrogen-bonded species) at the end of the  $T_w$  period (the time of the third pulse) that were also complexes immediately after the second pulse (peak (2625.6  $\text{cm}^{-1}$ , 2625.6  $\text{cm}^{-1}$ ) in the right panel of Figure 4). CF represents the free phenol molecules at the end of the  $T_w$  period that were complexes immediately after the second pulse (peak (2625.6  $\text{cm}^{-1}$ , 2666  $\text{cm}^{-1}$ ) in the right panel of Figure 4). The rate constant for dissociation of complexes is  $k_d$ , and the rate constant for the association of a free phenol with benzene or a benzene derivative to form a complex is  $k_a$ . During the  $T_w$  period, the vibrational echo signals produced by these two populations decrease because of vibrational relaxation (time constant  $T_c$  and  $T_f$  for complex and free, respectively) and rotational relaxation (time constant  $\tau_c$  and  $\tau_f$  for complex and free, respectively). Identical considerations apply to the populations FF and FC, which are the initial diagonal free population that is also free at  $T_w$  and the initial free population is complexed at  $T_w$ .

The kinetic model gives rise to a set of differential equations for the four populations, CC, CF, FF, and FC. These differential equations have been used previously,<sup>9,10,14</sup> and the complete

solutions have been published.<sup>10,14</sup> In the equations, only  $k_a$  and  $k_d$  are unknown variables; all of the other parameters are experimentally measured independently. Vibrational and rotational relaxation time constants were measured with pump–probe experiments as described in Experimental Procedures (section II). The time-dependent populations were provided by the peak volumes or intensities of the 2D-IR spectra corrected for transition dipole moment differences.<sup>9,10,14</sup> The transition dipole moment differences of the free and complexed species were measured using FT-IR. The equilibrium constant for the two species was also given by FT-IR measurements. The dissociation rate (number per unit time) of the complex equals the formation rate because the system is in equilibrium (see below).<sup>9</sup> The complex dissociation time constant (also the lifetime of the hydrogen bond),  $\tau_d$  (given in picoseconds below), is independent of concentration. Therefore,  $\tau_d$  is reported and discussed.  $\tau_d = 1/k_d$ , where  $k_d = k_d/A$  is the dissociation rate constant.  $A$  is the concentration ratio between the complexed and free phenol (or phenol derivative). The dissociation rate is  $k_d[\text{complex}]$ . Because the concentration ratio is known, there is a single unknown parameter,  $\tau_d$ .

Spectral diffusion changes the shape of the diagonal peaks, reducing their maximum amplitudes without changing their volumes. For this reason in previous publications<sup>9,10,14</sup> peak volumes were determined as a function of  $T_w$  to reflect the peak populations. Here we use amplitudes as a function of  $T_w$  instead of volumes when fitting the data with the kinetic model for all samples except the oMPH in TL/ $\text{CCl}_4$  system because the spectral diffusion is fast compared to the exchange rates. Therefore, negligible error is introduced by using the amplitudes, which are more easily determined than the volumes. For oMPH in TL/ $\text{CCl}_4$  peak volumes were used.

The data were fit in the following manner. For a 2D-IR spectrum taken at  $T_w = 200$  fs, the population ratio of the two species is taken to be the same as the equilibrium constant obtained from the FTIR measurements because 200 fs is a very short time compared to the time scale of chemical exchange. All of the free diagonal peaks are divided by the intensity of the free peak at 200 fs to yield the time-dependent populations

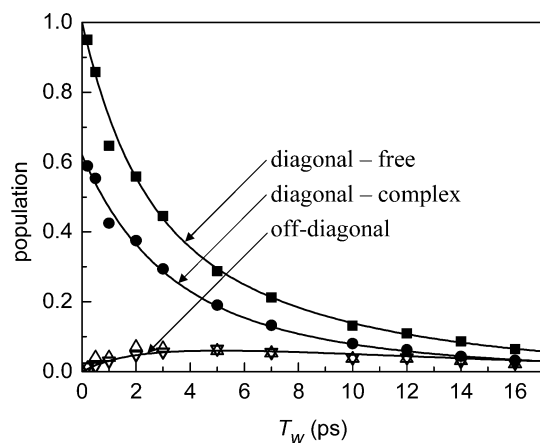


**Figure 6.**  $T_w$ -dependent data (symbols) showing the time dependence of the two diagonal and two off-diagonal peaks, in the 0–1 region of the 2D vibrational echo spectra as in Figure 5. The off-diagonal peaks grow in together because the sample is in thermal equilibrium. The solid curves are from a fit to the data with one adjustable parameter,  $\tau_d$ , using the kinetic model. Other parameters in the model are determined from independent experiments. For the phenol/toluene system  $\tau_d = 15 \pm 3$  ps.

for free phenol molecules (FF). All of the diagonal peaks for the complexes are divided by the intensity of the complex peak at 200 fs and then multiplied with the equilibrium constant to give the time-dependent populations of complexed phenol molecules (CC). This procedure accounts for the fact that the transition dipole moments of the free and complex species are not the same. The diagonal peak amplitudes depend on the fourth power of their respective transition dipoles. The off-diagonal peak amplitudes depend on the product of the squares of the transition dipoles of the free and complex species. To take this into account, the cross-peaks are divided by the square root of the intensity ratio of the complexed peak intensity over the free peak intensity divided by the equilibrium constant. The influence on the peak amplitudes caused by peak overlap is corrected for by fitting the 2D-peaks and subtracting the contributions to a given peak from the other peaks. This is a relatively small correction. The results yield the diagonal populations, FF and CC and the off-diagonal exchanged populations, CF and FC, as a function of  $T_w$ .

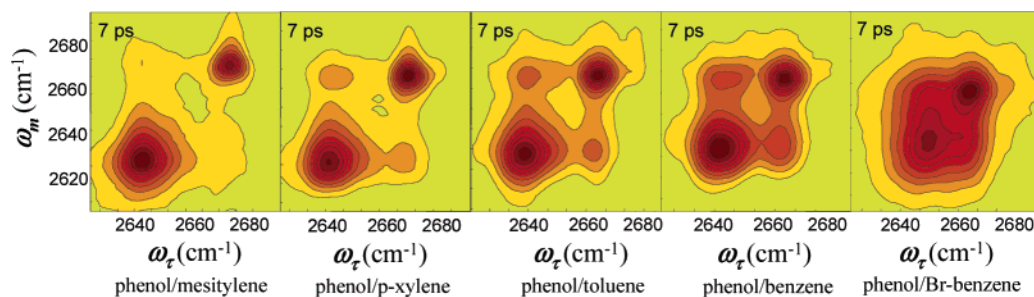
The data (see Figure 5 as an example) for the 0–1 transition region consist of four time-dependent components: the two diagonal peaks (the complex and the free PH in Figure 5) and the two off-diagonal peaks (dissociation and formation of the complex during the  $T_w$  period). As  $T_w$  increases, the off-diagonal peaks grow in because of chemical exchange. All four peaks can be reproduced with the single adjustable parameter,  $\tau_d$  by inputting the known constants and fitting the data with the kinetic equations. For the phenol/toluene system, the input parameters used are  $T_c = 10$  ps,  $T_f = 9$  ps,  $\tau_c = 3.7$  ps,  $\tau_f = 2.4$  ps, and the ratio of the complexed and free phenol concentrations [complex]/[free] = 0.62. Because the vibrational and rotational parameters were measured in pure solvents rather than mixtures, we allowed each parameter to vary  $\sim 10$ –20% in fitting the data and used the results to determine the error bars for  $\tau_d$ .

Figure 6 shows the peak intensity data for the 0–1 transition region of the spectrum as a function of  $T_w$ . The data are normalized to the largest peak at  $T_w = 0$ . The simultaneous fit (solid curves) to the time dependence of all of the peaks using a single adjustable parameter,  $\tau_d$ , is very good. From the fits,

the dissociation time for the PH/TL complex (hydrogen bond lifetime) is  $\tau_d = 15 \pm 3$  ps. To test the fitting procedures, the peak volumes were also fit for several of the samples. Within experimental error, the intensity fitting results for PH/BrBZ, PH/BZ, and PH/pX are identical to the volume fitting results.<sup>9</sup> Fits such as those displayed in Figure 6 for the phenol/toluene system are shown for all of the other samples in the Supporting Information.

In the analysis of the data presented in Figure 6 and for all of the other systems, it was assumed that the equilibrium between the complex and the free species and the exchange rates were not disturbed by the experiment. This assumption is supported by strong experimental evidence. First, if the system is in equilibrium, the two off-diagonal peaks will grow in at the same rate because the rate of complex formation is equal to the rate of complex dissociation. Within experimental error, the off-diagonal peaks grow in at the same rates as can be seen in Figure 6 for the phenol/toluene system and in the Supporting Information for all of the other systems.

Another detailed test showing that the vibrational echo/chemical exchange experiment does not perturb either the thermal equilibrium or the exchange rates has been presented for the phenol/benzene system.<sup>9</sup> The test involves comparing the 0–1 data, such as those shown in Figure 5, to the equivalent data for the 1–2 transition (not shown). There are two quantum pathways that give rise to the 0–1 2D spectrum. For one pathway, the system is in the ground state ( $\nu = 0$ ) during the  $T_w$  period. For the other pathway the system is in the vibrationally excited state ( $\nu = 1$ ) during the  $T_w$  period. Fifty per cent of the signal arises from each of these pathways. For the 1–2 portion of the 2D vibrational echo spectrum (see data in Supporting Information), there is only one pathway, and the first two radiation field–matter interactions the same as those that give rise to the vibrationally excited portion of the 0–1 2D spectrum. After the second interaction (second pulse) the system is in the  $\nu = 1$  state. The third interaction (third pulse) produces a coherence between the  $\nu = 1$  and  $\nu = 2$  levels, and the vibrational echo is then emitted at the frequency of the 1–2 transition, which is shifted to lower frequency by the vibrational anharmonicity ( $\sim 100$   $\text{cm}^{-1}$ ). The portion of the 2D spectrum that occurs from vibrational echo emission at the 1–2 frequency only involves a pathway in which the system is in the  $\nu = 1$  state during the  $T_w$  period. Therefore, the 0–1 portion of the spectrum involves 50% of the signal in which the dynamics might be influenced by vibrational excitation, whereas the 1–2 portion of the spectrum involves 100% of the signal that might be affected by vibrational excitation. It was observed that the measured dynamics are the same for the 0–1 and 1–2 portions of the spectrum.<sup>9</sup> Therefore, vibrational excitation does not influence the thermal equilibrium/chemical exchange rates. Vibrational excitation of the hydroxyl stretch is actually a very mild perturbation of the system. The hydroxyl stretch is a quantum oscillator. Vibrational excitation to the  $\nu = 1$  state increases the bond length by a few hundredths of an angstrom. This is a very small change compared to the thermal structural fluctuations of the complex (distance and angular) displayed in the MD simulations.<sup>19</sup> It should also be noted that the energy deposited by vibrational relaxation does not enter into the problem. Once a molecule undergoes vibrational relaxation, it no longer contributes to the signal.



**Figure 7.** 2D-IR vibrational echo spectra of the OD stretch of phenol in a series of mixed benzene derivative/ $\text{CCl}_4$  solvents with the same reaction time period,  $T_w = 7$  ps. The data have been normalized to the largest peak for each sample. Each contour represents a 10% change in amplitude. From left to right the hydrogen bonds are weaker, and the size of the off-diagonal peaks are larger (more exchange).

The hydrogen bond strength (bond formation enthalpy) of the complex is changed by modifying the chemical structure of the solute molecule, the solvent molecule, or both. It has been qualitatively demonstrated that stronger hydrogen bonds dissociate more slowly.<sup>9</sup> Here a more detailed and quantitative correlation is presented. Before discussing the values of the dissociation times, the nature of the results can be seen qualitatively and directly from the data presented in Figure 7. Figure 7 displays 2D-IR spectra for the same reaction period,  $T_w = 7$  ps, for complexes between phenol and five different complex partners in mixed solvents of each partner and  $\text{CCl}_4$ . The data have been normalized to the largest peak for each sample. Phenol forms the strongest hydrogen bond with mesitylene. The hydrogen-bond strength order is phenol/mesitylene > phenol/*p*-xylene > phenol/toluene > phenol/benzene > phenol/bromobenzene. In Figure 7, moving from left to right, it can be seen that at the single  $T_w = 7$  ps, the size of the off-diagonal peaks, which are produced by chemical exchange, increases as the hydrogen-bond strength decreases. For the phenol/mesitylene spectrum, the off-diagonal peaks have just begun to appear. In contrast, in the phenol/bromobenzene spectrum, the off-diagonal peaks have grown in to such an extent that they are now well delineated from the diagonal peaks and the spectrum has the appearance that is approximately square. As discussed above, exchange is the only reason for the growth of the off-diagonal peaks. Faster exchange produces larger off-diagonal peaks (normalized to the largest diagonal peak) for the same reaction period ( $T_w$ ). From the relative intensity of the cross-peaks (the number of contours), it is straightforward to see that a stronger hydrogen bond dissociates more slowly. Figure 7 is a demonstration that the stronger the hydrogen bond that forms the complex, the slower the dissociation and formation of the complex.

The enthalpies and entropies of complex formations were determined from the temperature dependence of the equilibrium constant using

$$\ln K_{\text{eq}} = -\frac{\Delta G^0}{RT} = -\frac{\Delta H^0}{RT} + \frac{\Delta S^0}{R} \quad (3)$$

The details are discussed in the Supporting Information.  $\Delta G^0$ ,  $\Delta H^0$ , and  $\Delta S^0$  are the standard Gibbs free energy, the enthalpy, and the entropy at room temperature, respectively. The standard state is defined to be a pressure of 1 atm and a temperature of 25 °C.  $\Delta H^0$  and  $\Delta S^0$  are taken to be temperature independent within the 50 K range used in the studies. Figure 8 shows a very interesting correlation between the lifetimes of the complexes ( $1/k_d$ ,  $k_d$  is the hydrogen-bond dissociation rate constant)

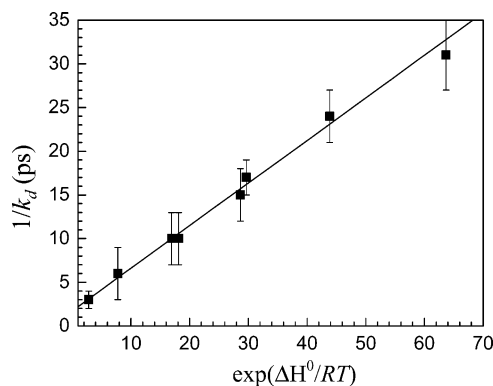


**Figure 8.** Hydrogen bond lifetimes ( $1/k_d$ , ps) plotted vs  $\exp(\Delta H^0/RT)$ —where  $\Delta H^0$  is the hydrogen-bond dissociation enthalpy (negative of the enthalpy of formation),  $R$  is the gas constant, and  $T$  is the temperature (300 K). The line through the data is given by eq 4.

and the dissociation enthalpies ( $\Delta H^0$ , negative values of the hydrogen-bond formation enthalpies) for the eight samples studied. The line through the data points is given by

$$1/k_d = B + A^{-1} \exp(\Delta H^0/RT), \quad (4)$$

where  $B = 2.3$  ps and  $A^{-1} = 0.5$  ps are constants. The equation can be rearranged to give

$$\frac{1}{1/k_d - B} = A \exp(-\Delta H^0/RT) \quad (5)$$

Since  $B = 2.3$  ps is smaller than or the same as the experimental errors for all of the samples except the fastest one, oMPH/TL, the relationship can be approximated for hydrogen bonds with lifetimes longer than 2.3 ps as

$$k_d = A \exp(-\Delta H^0/RT) \quad (6)$$

Equation 6 has the form of the Arrhenius equation<sup>28</sup> but with the dissociation enthalpy instead of the activation energy. It is useful to consider the trend seen in Figure 8 heuristically in terms of simple transition state theory.<sup>29</sup> The dissociation rate constant can be written as

(28) Atkins, P. W. *Physical Chemistry*, 5th ed.; W. H. Freeman: New York, 1994.

(29) Chang, R. *Physical Chemistry for the Chemical and Biological Sciences*; University Science Books: Sausalito, 2000.

$$k_d = \frac{k_B T}{h} \exp(-\Delta G^*/RT) = \frac{k_B T}{h} \exp(\Delta S^*/R) \exp(-\Delta H^*/RT) \quad (7)$$

where  $\Delta G^*$  is the activation free energy,  $\Delta S^*$  is the activation entropy, and  $\Delta H^*$  is the activation enthalpy. If the activation enthalpy is proportional to the dissociation enthalpy,  $\Delta H^* \propto \Delta H^0$ , and the activation entropy  $\Delta S^*$  is essentially a constant, independent of the molecular structure of the complexes, then eq 6 and the behavior displayed in Figure 8 are recovered.

Aside from experimental error, a possible explanation for the nonzero (2.3 ps) intercept in Figure 8 is the time required for the molecules of a hypothetical nonbonded complex to separate diffusively. Consider a “pseudocomplex” that has a bond formation enthalpy of zero but has a phenol derivative molecule and a benzene derivative molecule in the T-shaped structure of a bonded complex. For the phenol/benzene complex, detailed MD simulations show that the structure has significant angular fluctuation, but the average angle is  $90^\circ$ .<sup>19</sup> In the complexed form, the distance between the ring center of the benzene and the D atom of the OD group is  $\sim 2.5$  Å, but by  $\sim 3.5$  Å separation, the phenol and benzene are no longer bonded as shown by the lack of angular correlation.<sup>19</sup> For the pseudocomplex with zero bond formation enthalpy, it would still take a finite amount of time for the phenol and benzene to separate from  $\sim 2.5$  Å to  $\sim 3.5$  Å. The time to diffuse apart may be responsible for the nonzero intercept in Figure 8. As a very crude check of this idea, using the Stokes–Einstein equation and the viscosity of the benzene/ $\text{CCl}_4$  solvent, it was determined that the time for a benzene to diffuse 1 Å is  $\sim 2$  ps, consistent with the intercept. This is a very rough approximation for two reasons that tend to off-set each other. For two molecules in a solvent, the mutual diffusion constant is well approximated by the sum of the diffusion constants.<sup>30</sup> Therefore, the time for a phenol and a benzene to change their separation by 1 Å would be shorter than 2 ps. However, the mutual diffusion constant is only appropriate when the molecules are widely separated. At small separations, the hydrodynamic effect slows their relative diffusion.<sup>31–34</sup> These off-setting effects make the  $\sim 2$  ps estimate reasonable. The point is that the time scale to simply diffuse apart is not 0.2 ps or 20 ps, but on the order of the intercept in eq 4.

The correlation between the lifetimes of solute–solvent hydrogen bonds and their enthalpies of formation may be useful for estimating the lifetimes of hydrogen bonds that are similar

to those studied here. By combining eqs 1 or 2 with eq 6, a hydrogen bond lifetime can be roughly estimated from the OH or OD stretch frequency shift of the system obtained from routine FT-IR measurements.

#### IV. Concluding Remark

The study presented here extends previous work that examined hydrogen-bond formation and dissociation rates of the phenol/benzene complex.<sup>9,10</sup> Here, eight  $\pi$  hydrogen-bonded complexes of phenol and phenol derivatives with benzene and benzene derivatives were investigated. The series of complexes have a wide range of hydrogen-bond strengths (enthalpies of formation). Both the kinetics and thermodynamics of the complexes were studied. The 2D-IR vibrational echo experiments measure the dissociation and formation rates of the complexes. The chemical exchange dynamics of a complex can be characterized by the dissociation time of the complex (the inverse of the dissociation rate), which is the hydrogen bond lifetime. The measured dissociation times for the eight complexes range from 3 to 31 ps. The bond dissociation enthalpies (negative of the formation enthalpies) range from 0.6 kcal/mol to 2.5 kcal/mol.

It was found that the hydrogen bond lifetimes are correlated with the dissociation enthalpies in a manner akin to the Arrhenius equation. The correlation can be qualitatively understood in terms of transition state theory. In this model, the activation enthalpy scales linearly with the bond dissociation enthalpy, and the activation entropy is essentially independent of the molecular structure of the complex. It was also found that the shift in the hydroxyl stretch frequency of phenol and its derivatives when complexed, compared to that of the free species, is linearly related to the dissociation enthalpy. Thus, it is possible to estimate the hydrogen bond lifetimes of systems that are similar to those studied here from a simple measurement of the hydroxyl stretch frequency in a linear absorption experiment.

**Acknowledgment.** We thank Sunnam Park, Kyungwon Kwak, and David Ben Spry for their help with some of the pump/probe experiments and Dr. Xin Chen and Professor John I. Brauman for insightful discussions. This work was supported by grants from AFOSR (F49620-01-1-0018), NIH (2 R01 GM-061137-05), and NSF (DMR-0332692).

**Supporting Information Available:** Vibrational echo 2D-IR experimental setup and details, calculated structures of complexes, thermodynamic data, 2D-IR data and kinetic results of all samples. This material is available free of charge via the Internet at <http://pubs.acs.org>.

JA067760F

- (30) Swallen, S. F.; Fayer, M. D. *J. Chem. Phys.* **1995**, *103*, 8864–8872.  
(31) Wolynes, P. G.; Deutch, J. M. *J. Chem. Phys.* **1976**, *65*, 450–454.  
(32) Northrup, S. H.; Hynes, J. T. *J. Chem. Phys.* **1979**, *71*, 871–883.  
(33) Rice, S. A. *Diffusion-Limited Reactions*; Elsevier: Amsterdam, 1985.  
(34) Weidemaier, K.; Tavernier, H. L.; Swallen, S. F.; Fayer, M. D. *J. Phys. Chem. A* **1997**, *101*, 1887–1902.  
(35) Fuchs, R.; Peacock, L. A.; Stephenson, W. K. *Can. J. Chem.* **1982**, *60*, 1953–1958.